

Technical Report

TR-00-09

Study of creep behaviour in P-doped copper with slow strain rate tensile tests

Xuexing Yao, Rolf Sandström
Department of Materials Science and Engineering
Royal Institute of Technology (KTH)

August 2000

Svensk Kärnbränslehantering AB

Swedish Nuclear Fuel
and Waste Management Co
Box 5864
SE-102 40 Stockholm Sweden
Tel 08-459 84 00
+46 8 459 84 00
Fax 08-661 57 19
+46 8 661 57 19



Study of creep behaviour in P-doped copper with slow strain rate tensile tests

Xuexing Yao, Rolf Sandström
Department of Materials Science and Engineering
Royal Institute of Technology (KTH)

August 2000

Keywords: Creep, tensile test, slow strain rate, pure copper, phosphorous.

This report concerns a study which was conducted for SKB. The conclusions and viewpoints presented in the report are those of the author(s) and do not necessarily coincide with those of the client.

Abstract

Pure copper with addition of phosphorous is planned to be used to construct the canisters for spent nuclear fuel. The copper canisters can be exposed to a creep deformation up to 2–4% at temperatures in services. The ordinary creep strain tests with dead weight loading are generally employed to study the creep behaviour; however, it is reported that an initial plastic deformation of 5–15% takes place when loading the creep specimens at lower temperatures. The slow strain rate tensile test is an alternative to study creep deformation behaviour of materials. Ordinary creep test and slow strain rate tensile test can give the same information in the secondary creep stage. The advantage of the tensile test is that the starting phase is much more controlled than in a creep test. In a tensile test the initial deformation behaviour can be determined and the initial strain of less than 5% can be modelled. In this study slow strain rate tensile tests at strain rate of 10^{-4} , 10^{-5} , 10^{-6} , and 10^{-7} s⁻¹ at 75, 125 and 175°C have been performed on P-doped pure Cu to supplement creep data from conventional creep tests. The deformation behaviour has successfully been modelled. It is shown that the slow strain rate tensile tests can be implemented to study the creep deformation behaviours of pure Cu.

Table of contents

	page
1 Introduction	7
2 Testing procedure	9
2.1 Material specification	9
2.2 Tensile tests	10
2.3 Vickers hardness	10
2.4 Metallographic analysis	10
3 Results	11
4 Discussion	15
4.1 Creep behaviour of copper	15
4.2 Model for slow strain rate tensile tests	18
4.3 Comparison of the slow strain rate test data with the models	18
5 Conclusions	21
Acknowledgements	23
References	25

1 Introduction

The proposed method in Sweden for nuclear waste disposal involves the placement of the used fuel in cylindrical canisters with a diameter of about 0.9 m and a length of 5 m /1/. The outer and inner shells in the canisters are assumed to be made of copper and iron, respectively. Between the two shells there is an initial gap of 2 mm. The canisters are sealed with top end pieces of copper, which are electron-beam welded into place. The canisters are to be located in granitic rock with bentonite clay around them. The heat from the fuel elements will give rise to temperatures of up to 90°C for a period of several hundred years. From the ground water and the surrounding bentonite filler, the canisters will be exposed to an external pressure of up to 15 MPa. These conditions will cause creep deformation up to 5% strain in the copper before the gap between the shells is closed.

Initially oxygen-free high conductivity (Cu-OF) copper was considered due to its thermodynamic stability in ground water at the depth of a repository. Previously, the creep ductility of pure copper had been reported for temperatures from 350 to 500°C. For larger grain sizes $\geq 150 \mu\text{m}$, the creep ductility decreased with increasing grain size, and intergranular failure was observed /2, 3/. The lowest reported creep elongation was 6%. Only if dispersion strengthening is present, lower ductility down to 1% has been observed /4/. It is obvious that failure of canisters made of copper is not expected unless the creep ductility of copper is low. It is therefore necessary to study the creep behaviour of the copper specimens under laboratory conditions in order to advise on fabrication processes for the copper canisters to ensure longer service life and prolong the rupture life.

The obvious way of study the creep phenomenon of copper canisters is to perform ordinary creep strain tests with dead weight loading. A large number of such tests have and are being performed at the Swedish Institute for Metals Research /5-11/. Unfortunately it has turned out that when loading the creep specimens an initial plastic deformation of 5–15% takes place. This deformation is larger at lower than at higher temperatures. An alternative test method would be to use tensile tests with slow strain rates. Such tests are not very common due to lack of suitable equipment. The advantage with the tensile test is that the starting phase is much more controlled than in a creep test. The purpose of the present investigation is to perform slow strain rate tensile tests for P-doped copper to supplement creep data from conventional creep tests. A model for the slow strain rate tensile tests was used to simulate the test results.

2 Testing procedure

2.1 Material specification

The requirements and comments concerning chemical composition, grain size, and mechanical properties are shown in Table 2-1 according to the Technical Specification No KTS001 /12/ from Swedish Nuclear Fuel and Waste Management Co (SKB).

Table 2-1. Requirements and comments concerning chemical composition, grain size, and mechanical properties.

Requirements	Specification	Comments
Weldability	O<5 ppm	Higher levels give reduced weldability.
Ductility	H<0.6 ppm	Higher levels give reduced mechanical properties (Hydrogen embrittlement).
Tensile strength ductility	S<8 ppm	Higher levels give reduced mechanical properties caused by non-dissolved sulphur which will be concentrated to grain boundaries.
Creep ductility	P: 40–60 ppm	A phosphorus content of this order reduces the influence of sulphur impurities, increases creep ductility, increases recrystallization temperature and has a minor influence on the weldability.
	Grain size <360 µm (Plates or extrusion)	This grain size gives a resolution at ultrasonic testing comparable to X-ray testing of a 50 mm thick copper.
Ductility	Elongation > 40% RT-100°C (Plates or extrusion)	The canister will be deformed 4% in final repository.
Creep ductility	Elongation at creep rupture >10% RT-100°C (Plates or extrusion)	Same comments as above.

The material for copper canisters shall fulfil the specification in the standard UNS C10100 (Cu-OF, Table 2-2) or En 133/63:1994 Cu-OF1 (Table 2-3) with the following additional requirements: O<5 ppm, P 40-60 ppm, H<0.6 ppm, S<8 ppm and a grain size <360 µm.

Table 2-2. Rest elements in some commercial pure coppers (ppm).

	Ag	As	Fe	S	Sb	Se	Te	Pb	Bi	Cd	Mn	Hg	Ni	O	Sn	Zn
UNS C10100	25 ^b	5	10	15	4	3	2	5	1 ^b	1	0.5	1	10	5	2	1
EN133/63 Cu-OF1	25 ^b	5 ^c	10 ^d	15 ^b	4 ^b	2 ^e	2 ^f	5 ^b								

- b Maximum content
c $\Sigma (As+Cd+Cr+Mn+Sb) \leq 15$ ppm
d $\Sigma (Co+Fe+Ni+Si+Zn) \leq 20$ ppm
e $\Sigma (Bi+Se+Te) \leq 3.0$ ppm
f $\Sigma (Se+Te) \leq 3.0$ ppm

In this study, pure copper with addition of 50-ppm phosphorous is used throughout the tests.

2.2 Tensile tests

Specimens with cylindrical cross section, 10 mm in diameter and 50-100 mm in gauge were used. The performed tests are listed in the Table 2-3.

Table 2-3. Slow strain rate tensile test matrix.

Strain rate, /s	75°C	125°C	175°C	Max strain
1x10 ⁻⁴	*	*	*	—
1x10 ⁻⁵	*	*	*	—
1x10 ⁻⁶	*	*	*	5%
1x10 ⁻⁷	*	*	*	5%

2.3 Vickers hardness

Vickers hardness values on the received material bar were measured with 50-g load and 10-s dwell time in a digital micro-hardness tester (Future-Tech Corp., Japan). Ten measurements were performed and the averaged hardness value was obtained.

2.4 Metallographic analysis

Specimens for metallography were sectioned longitudinally, ground and polished and then given a final polish in a paste made from MgO and boiled distilled water with a few drops of glycerol and ammonia. The specimens were etched in ferric chloride. The microstructure of as received material, specimens tested at 175°C and 10⁻⁷ s⁻¹ and at 75°C and 10⁻⁴ s⁻¹ was then examined.

3 Results

The average (micro) Vickers hardness value was found to be 116 HV. The microstructure was studied before testing in a light optical microscope and is shown in Figure 3-1. The grain size was determined to be 180 μm . Figure 3-2 and Figure 3-3 show the microstructure of specimens deformed to 5% at a strain rate of 10^{-7} s^{-1} and 175°C and to failure at a strain rate of 10^{-4} s^{-1} and 75°C, respectively. Creep cavities have not been detected in the deformed structure even at lowest strain rate and highest test temperature (Figure 3-2). In addition, very little grain boundary damage can be seen even in specimens tested to failure (Figure 3-3).

However, a characteristic creep behaviour is demonstrated during the slow strain rate tensile tests with a constant engineering stress in the plastic range. The stress strain curves generated at different temperature and at strain rate of 10^{-4} s^{-1} and 10^{-7} s^{-1} are shown in Figure 3-4 and Figure 3-5, respectively. It is noted that a conventional stress-strain curve at room temperature is observed compared with the genuine creep behaviour at higher temperatures with a constant engineering stress. The yield strength, tensile strength and elongation at room temperature, see Figure 3-4 are consistent with properties after 10% cold working (Metals Handbook). This corresponds to 1/8 hard temper, which is referred to as H00 in the ASTM designation scheme.

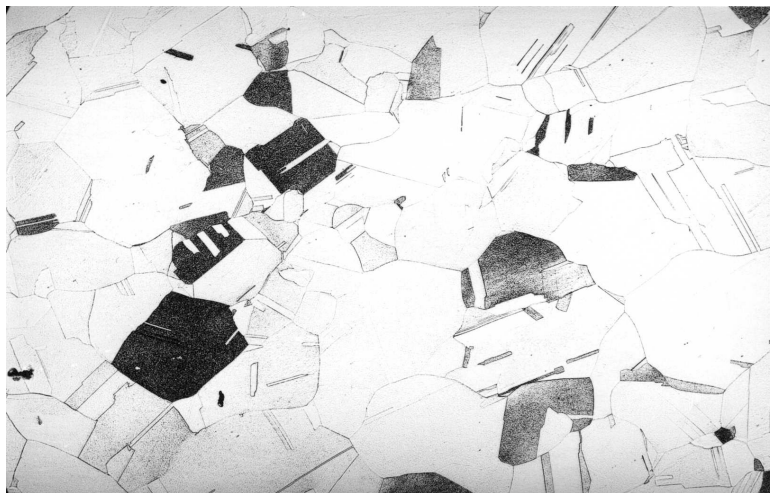


Figure 3-1. The microstructure of the test material as received state. (100x)

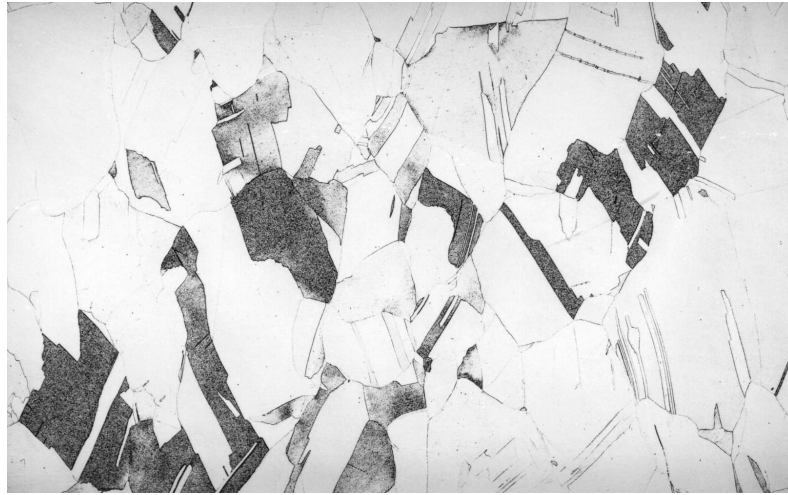


Figure 3-2. Longitudinal section of specimen tested till 5% strain at 175°C and $10^7 s^{-1}$. (100x)



Figure 3-3. Longitudinal section of specimen tested till fracture at 75°C and $10^4 s^{-1}$. (100x)

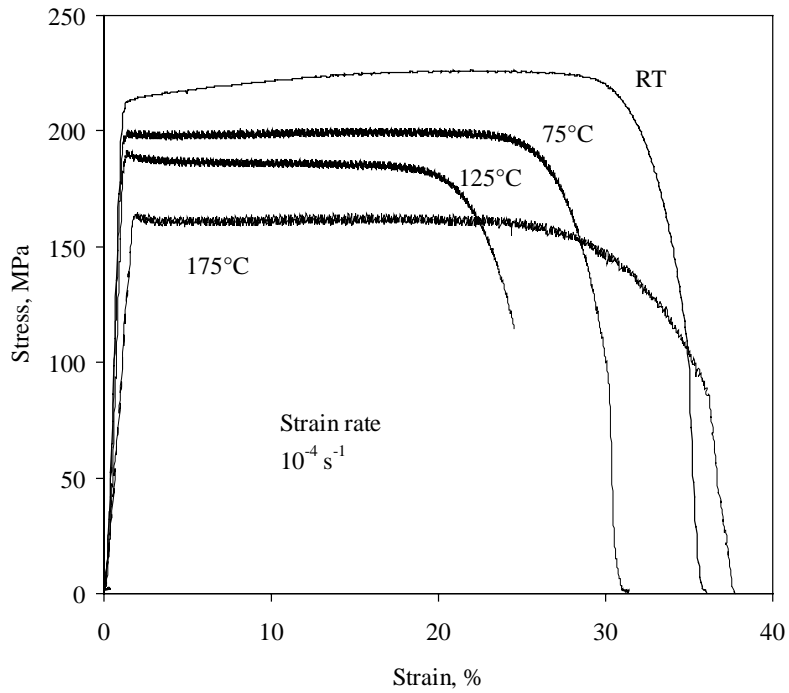


Figure 3-4. Stress-strain curves generated at a strain rate of $10^{-4}/\text{s}$ at different temperatures. The test at room temperature was performed at $10^{-3}/\text{s}$.

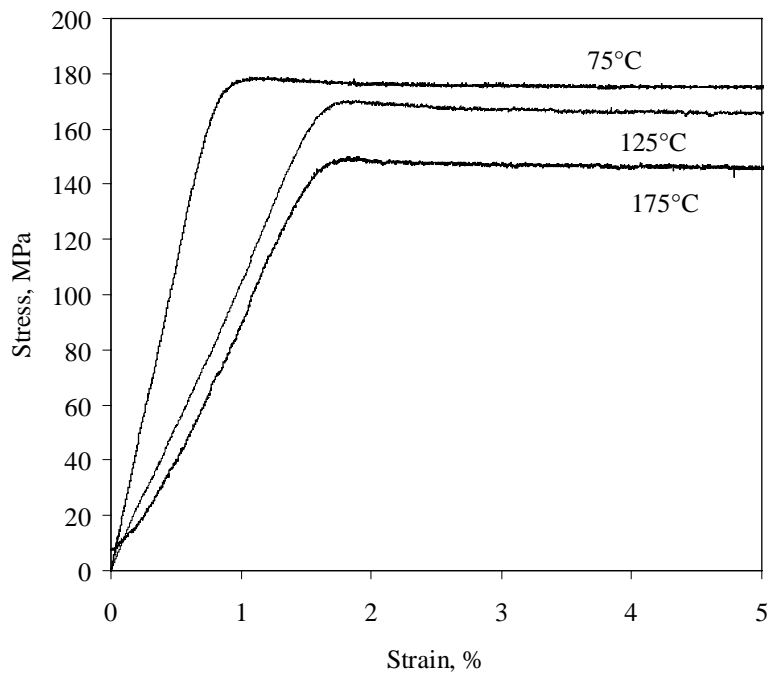


Figure 3-5. Stress-strain curves generated at a strain rate of $10^7/\text{s}$ at different temperatures.

4 Discussion

4.1 Creep behaviour of copper

The steady-state creep rate,

$$\dot{\epsilon}$$

of pure metals has been well characterised, so that in at low and intermediate stresses it is generally represented by a relationship of the form

$$\dot{\epsilon} = A(DGb/kT)(\sigma/G)^n \quad (4-1)$$

where D is the self diffusion coefficient ($D = D_0 \exp(-Q_c / RT)$), where D_0 is the frequency factor, Q_c is the activation energy for creep and R is the universal gas constant), G is the shear modulus, b is the Burgers vector, k is Boltzmann's constant, and A , and n are dimensionless constants. The value of n is usually increasing with decreasing temperature and increasing stress. For pure metals deforming in power-law creep regime the stress exponent, n , is in the range ~4–7.

At intermediate temperatures in the range ~0.4–0.7 T_m , the climb rate is controlled by vacancy diffusion in the lattice. At lower temperatures the dominating diffusion process is pipe diffusion along dislocation cores /14/. These two processes are sometimes termed high temperature climb and low temperature climb, respectively. The difference in diffusion process affects the activation energy. The activation energy for pipe diffusion is significantly lower than that of volume diffusion.

Table 4-1 summarises the creep data for copper, including purity, grain size, range of homologous temperature, range of normalised stress, reported stress exponent, and the value of the ratio Q_c / Q_l where Q_c is the reported activation energy for creep and $Q_l = 210 \text{ kJ/mol}$. The creep behaviour of copper can be described by the power-law relation at high temperature and at low stress /17, 18, 20-23/. The power-law breakdown at low temperature and high stress is also reported /5, 6, 9, 13, 19/. For P-free copper the transition takes place at about 100 MPa and 160 °C /5/. For P-doped Cu the transition can be expected to take place at higher temperatures. n values in the range of 35 to 73 have been measured on P-doped copper by Andersson, Seitisleam and Sandström /13/ at 175°C. Thus it is well known for copper in the same way as for steels that the stress exponent increases dramatically with decreasing temperature and increasing stress often reaching values in the range 50-100 /5, 13/. This is referred to as power-law break down (somewhat artificially since Eqn. (4-1) is still satisfied).

If the stress exponent, n , is evaluated from the tensile tests in the same way as for creep data /6, 9, 13, 20–25/, it can be obtained from Figure 4-1. n is fairly independent of test temperature and takes values around 65. In Figure 4-2 the results at 175°C from the tensile tests are compared to creep test results at the same temperature /13/. Creep data are available for three phosphorous contents 30, 60 and 110 ppm. Increasing the P-content from 0 to 30 ppm has a dramatic effect on the creep rate but an increased content above that level has only a marginal effect /13/. The tensile test results are

Table 4-1. A compilation of creep data for copper.

Purity	d (μm)	T/T_m	$\sigma/G(x10^{-4})$	n	Q_c/Q_i	Reference
Cu-OF	20	0.26–0.35	17.2–66.8	–	0.73	Tietz and Dorn /15/
Cu-OF	20	0.05–0.26	66.8–89.0	–	0.10–0.73	Landon et al /16/
99.990	30	0.50	6.8–27.7	4.6	0.55–0.63	Feltham et al /17/
		0.53	5.0–22.3	4.4		
		0.57	3.8–14.1	5.8		
		0.61	3.4–15.4	4.3		
		0.67	1.7–6.7	2.8		
		0.67	6.7–13.9	4.9		
		0.72	4.5–9.7	4.7		
99.995	30	0.57	6.0–14.0	4.8	0.55	Barrett and Sherby /18/
	30	0.64	6.3–9.5	4.8	0.55	
	1000	0.85	1.0–1.7	4.8	1.00	
99.950	30	>0.85	2.7–5.5	>7	3.30	Gilbert and Munsom /19/
		0.75–0.85	2.5–5.1	>7	1.50	
		0.74	4.8	4.5	0.48	
99.990	450	0.50	4.1–19.1	5.9		Pahutová et al /20/
		0.53	4.2–19.5	6.3	0.5–1.0	
		0.57	2.9–20.0	6.3		
		0.61	2.9–20.5	6.3		
		0.64	2.0–15.0	6.3	1.2–2.0	
		0.68	2.0–11.6	6.1		
		0.72	2.1–11.9	6.3		
		0.75	3.3–8.1	6.3		
99.990	500	0.45	10.0–25.0	7.2	–	Okrainets and Pischak /21/
		0.56	3.4–15.6	4.9	–	
		0.68	8.3–4.2	4.0	–	
99.998	400	0.61–0.73	3.3–4.5	3.7–4.0	0.66–2.67	Retima and Cornet /22/
97.880	250	0.46–0.72	0.0003–0.002	4.2–6.6	0.64–0.86	Raj and Langdon /23/
Cu-OF	45–115	0.36–0.40	0.002–0.00255	10.2–15.0	–	Lindblom et al /9/
Cu-OF	–	0.26–0.31	0.00186–0.0041	10.42–26.77	–	Ivarsson et al /6/
Cu-OF	100–2000	0.33	0.003–0.004	14–73	–	Andersson et al /13/

within the scatter band of the creep data albeit on the higher side. The slope of the curves (stress exponent) is about the same. It can hence be confirmed that there is an acceptable agreement between the two test methods. It is interesting to note that the amount of scatter in the tensile data is lower than that in the creep results. The reason is probably that the initial phase of the tensile tests is more controlled than in the creep tests.

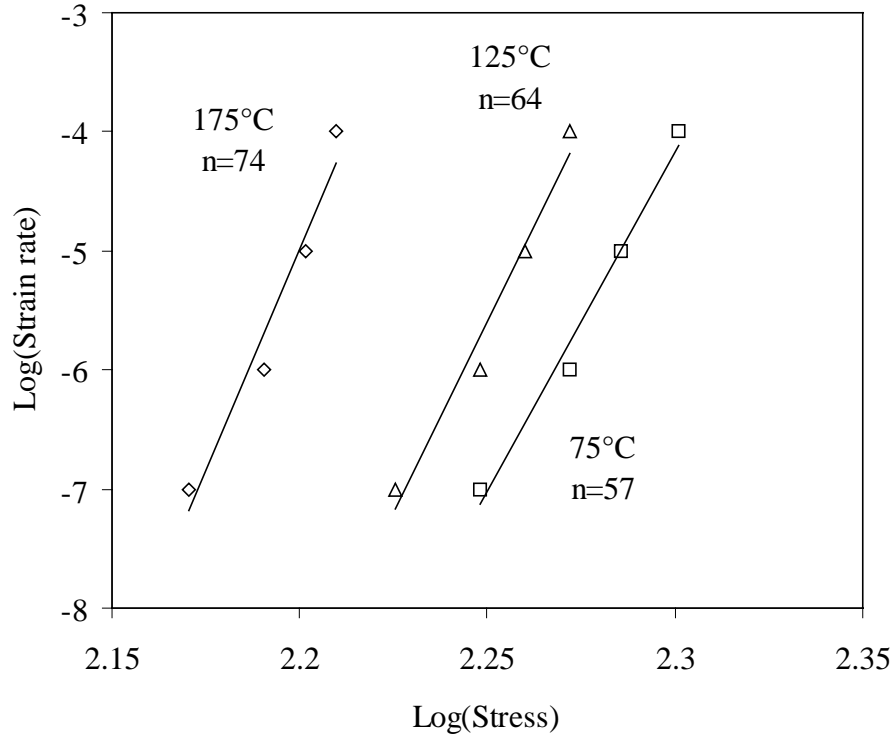


Figure 4-1. Stress vs. strain rate at different test temperatures. The stress exponent at each temperature is given.

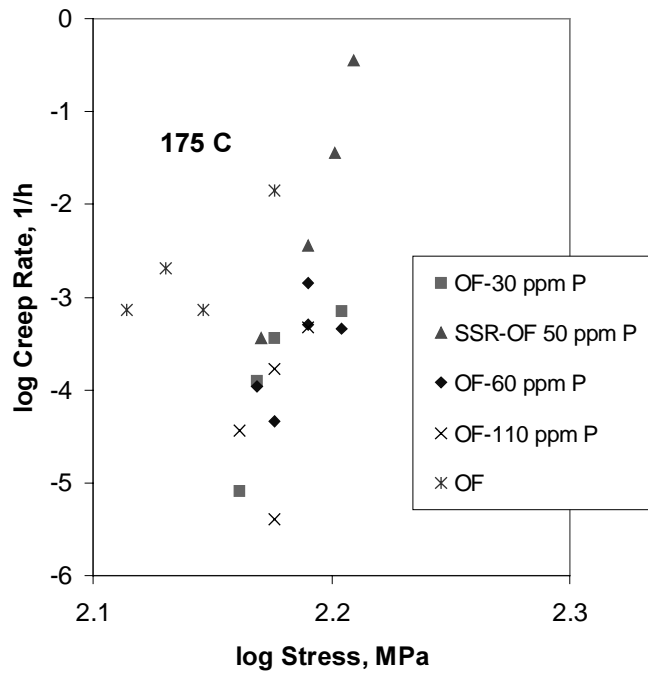


Figure 4-2. Strain rate as a function of stress for the slow strain rate tensile test (SSR-OF 60 ppm) and the minimum creep rate versus stress for creep tests for three P-contents 0, 30, 60 and 110 ppm /13/.

4.2 Model for slow strain rate tensile tests

In any tensile tests, both elastic and plastic strains have a central role in the deformation process. In addition, at higher temperatures creep deformation is of importance. It is well established that power law creep deformation takes place at temperatures as low as 75°C in pure copper /5/. An estimate of the dislocation climb rate taking deformation enhanced vacancy formation into account shows that the climb rate is high enough down to 75°C to control the creep rate.

The three types of deformation mechanisms are modelled in the following way. The total strain rate is taken as the sum of the elastic strain rate and the creep rate.

$$\dot{\epsilon}_{tot} = \frac{\dot{\epsilon}}{E_{app}} + A(\sigma - \sigma_i)^n \quad (4-2)$$

where the back stress σ_i is given by

$$\sigma_i = \sigma_{i0} + H\left(1 - \frac{\sigma}{\sigma_{max}}\right)\epsilon \quad (4-3)$$

E_{app} is the apparent elastic modulus. It is primarily controlled by the stiffness of the testing machine, which varies between tests. The two terms on the right hand side of Eqn.(4-3) represent the back stress from the lattice and the dislocation substructure respectively. H is an apparent work hardening rate. σ_{max} is the maximum stress that can be reached due to dynamic recovery. It is well established that a pronounced substructure is formed during deformation at creep rates at lower temperatures /24/. Eqn. (4-3) has a similar form as the Kocks-Mecking model for work hardening /25/. Eqn. (4-2) is solved with numerical integration with respect to time.

4.3 Comparison of the slow strain rate test data with the models

The slow strain rate test data are compared with the model in Figures 4-3 through 4-5 for 10^{-3} s^{-1} at 20°C, for 10^{-4} s^{-1} at 75°C as well as for 10^{-7} s^{-1} at 175°C. Both curves representing true and engineering stresses and strains are given. The engineering data are more directly comparable to conventional creep tests, whereas the true data are more appropriate for analysis with the model. The engineering stresses have consequently been used in Figures 4-1 and 4-2. The model reproduces the observed values quite accurately. A stress exponent of $n = 65$ has been used. Both the sharp transitions from the elastic to the creep range as well as the almost linear increase in stress with strain in the latter range are well described. The agreement is as accurate in all the other cases studied.

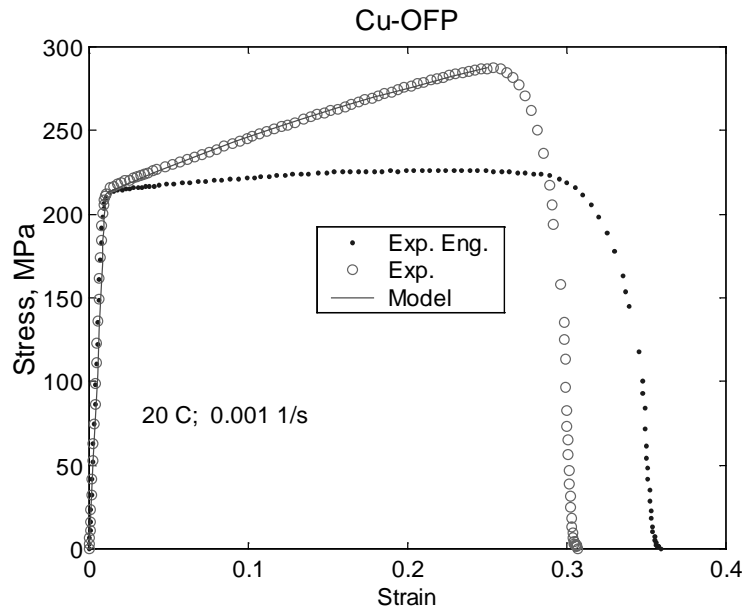


Figure 4-3. Stress versus strain for a strain rate of 0.001/s at 20°C. P-doped copper. Model values are compared to the true stress-strain curve. The engineering stress-strain curve is given for reference.

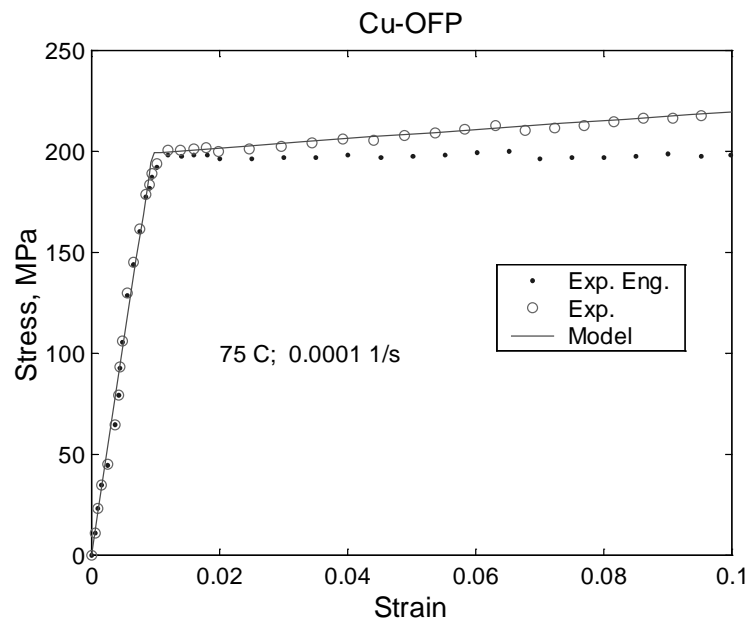


Figure 4-4. Stress versus strain for a strain rate of 0.0001/s at 75°C. P-doped copper. Model values are compared to the true stress-strain curve. The engineering stress-strain curve is given for reference.

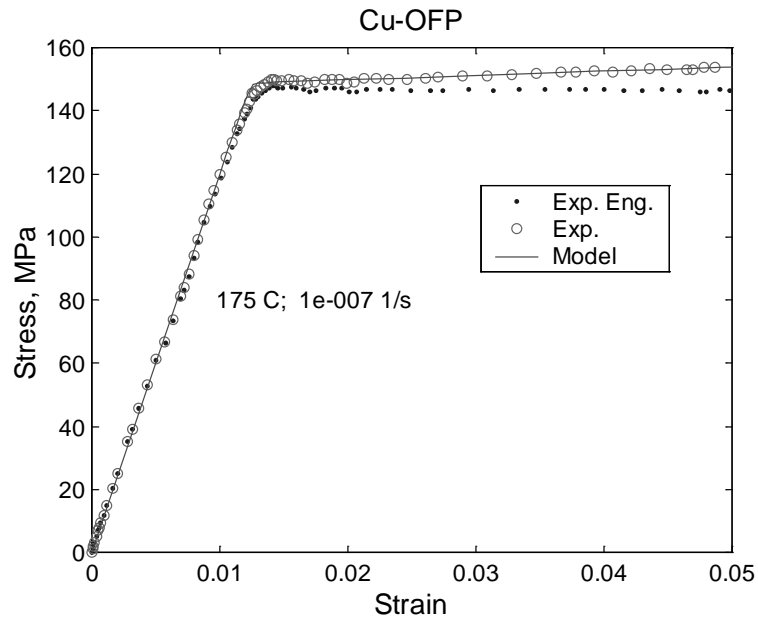


Figure 4-5. Stress versus strain for a strain rate of 10^{-7} 1/s at 175°C. P-doped copper. Model values are compared to the true stress-strain curve. The engineering stress-strain curve is given for reference.

The “work hardening” rate H takes values in the range from 300–400 MPa at 10^{-4} 1/s to 100–200 MPa at 10^{-7} 1/s with the higher and lower values at 75 and 175°C, respectively. This variation is expected since the recovery increasing with increasing temperature and it has more time to be active at low strain rates. The H value at 20°C is 750 MPa and consequently much higher than at elevated temperatures.

At high temperatures there is a slight tendency to a yield point. The increase in creep strength due to alloying with phosphorous is a result of solute drag, i.e. a partial locking of the dislocations due an enrichment of P-atoms at the dislocation cores. Such enrichment often appears as a yield point as well.

5 Conclusions

Slow strain rate tensile tests at strain rates in the range 10^{-4} to 10^{-7} s⁻¹ at 75, 125 and 175°C have been performed on P-doped pure Cu to supplement data from conventional creep tests. It is confirmed that ordinary creep test and slow strain rate tensile test give consistent information in the secondary creep stage. The slow strain rate tensile test is an alternative to the ordinary creep test with the advantage of the starting phase is much more controlled than in a creep test.

A model for the slow strain rate tensile curves has been formulated. Precise agreement between the modelled curves and experimental data has been achieved.

Acknowledgements

X X Yao would like to thank Professor Rolf Sandström for hospitality at the Department of Materials Science and Engineering, Royal Institute of Technology, Stockholm. This project was funded by Swedish Nuclear Fuel and Waste Management Co (SKB), Stockholm, Sweden. SKB also supplied the material.

References

1. SKB Annual Report 95. TR 95-37, Swedish Nuclear Fuel and Waste Management Co, 1996.
2. **Tipler H R, McLean D.** *Met. Sci. J.*, 4, 103–107, 1970.
3. **Fleck R G, Cocks G J, Taplin D M R.** *Metall. Trans.*, 1, 3415–3420, 1970.
4. **Rigollet C, Gentzbittel J M, Robert G, de Phys J.** *IV, Colloque C7 Suppl. 3*, 747–750, 1993.
5. **Henderson P J, Sandström R.** *Mater. Sci. Eng.*, A246, 143–150, 1998.
6. **Ivarsson B G, Österberg J-O.** Swedish Institute for Metals Research, Stockholm, Report IM-2384, 1988.
7. **Henderson P J, Österberg J-O, Ivarsson B G.** Swedish Institute for Metals Research, Stockholm, Report IM-2780, 1991.
8. **Henderson P J.** Swedish Institute for Metals Research, Stockholm, Report IM-3112, 1994.
9. **Lindblom J, Henderson P J, Seitisleam F.** Swedish Institute for Metals Research, Stockholm, Report IM-3197, 1995.
10. **Seitisleam F, Henderson P J, Lindblom J.** Swedish Institute for Metals Research, Stockholm, Report IM-3327, 1996.
11. **Seitisleam F, Henderson P J.** Swedish Institute for Metals Research, Stockholm, Report IM-3506, 1997.
12. Technical Specification No KTS001 – Material for Copper Canisters, Swedish Nuclear Fuel and Waste Management Co (SKB), 1998.
13. **Andersson H, Seitisleam F, Sandström R.** Swedish Institute for Metals Research, Stockholm, Report IM-1999-0701, 1999.
14. **Robinson S L, Sherby O D.** *Acta Metall.*, 17, 109, 1969.
15. **Tietz T E, Dorn J E.** *Trans. Amer. Inst. Min. Eng.*, 206, 156, 1956.
16. **Landon P R, Lytton J L, Shepard L A, Dorn J E.** *Trans. Amer. Soc. Metals*, 51, 900, 1958.
17. **Feltham P, Meakin J D.** *Acta Metall.*, 7, 614, 1959.
18. **Barrett C R, Sherby O D.** *Trans. Amer. Inst. Min. Eng.*, 230, 1322, 1964.

19. **Gilbert E R, Munson D E.** Trans. Amer. Inst. Min. Eng., 233, 429, 1965.
20. **Pahutová M, Cadek J, Ryš P.** Phil. Mag., 23, 509, 1971.
21. **Okrainets P N, Pischak V K.** Phys. Metals Metallogr., 46, 123, 1979.
22. **Retima M, Cornet M.** Acta Metall., 34, 753, 1986.
23. **Raj S V, Langdon T G.** Acta Metall., 37, 843, 1989.
24. **Straub S, Blum W, Maier H J, Ungár T, Borbély A, Renner H.** Acta Mater. 44, 4337–4350, 1996.
25. **Kocks F, Mecking H.** Acta Metall. 29, 1865, 1981.